Securing Transient Stability Using Time-Domain Simulations Within an Optimal Power Flow

Rafael Zárate-Miñano, *Student Member, IEEE*, Thierry Van Cutsem, *Fellow, IEEE*,
Federico Milano, *Senior Member, IEEE*, and Antonio J. Conejo, *Fellow, IEEE*

Abstract—This paper provides a methodology to restore transient stability. It relies on a well-behaved optimal power flow model with embedded transient stability constraints. The proposed methodology can be used for both dispatching and redispatching. In addition to power flow constraints and limits, the resulting optimal power flow model includes discrete time equations describing the time evolution of all machines in the system. Transient stability constraints are formulated by reducing the initial multi-machine model to a one-machine infinite-bus equivalent. This equivalent allows imposing angle bounds that ensure transient stability. The proposed optimal power flow model is tested and analyzed using an illustrative nine-bus system, the well-known New England 39-bus system, a ten-machine system, and a real-world 1228-bus system with 292 synchronous machines.

Index Terms—Dispatching, optimal power flow, redispatching, single-machine equivalent, transient stability.

NOTATION

THE main notation used throughout the paper is stated below for quick reference. Other symbols are defined as needed throughout the paper.

A. Functions

$f(\cdot)$	Cost function.
$I_{nm}(\cdot)$	Current magnitude from bus n to bus m as a function of state variables.
$P_{nm}(\cdot)$	Active power flow from bus n to bus m as a function of state variables.
$Q_{nm}(\cdot)$	Reactive power flow from bus n to bus m as a function of state variables.

B. Variables

E'_i	Emf magnitude of generator i.
P_{ei}	Electrical power of generator i.

P_{Gi}	Active power production of generator i.
P_{Gn}	Total active power production in bus n.
Q_{Gi}	Reactive power production of generator i.
Q_{Gn}	Total reactive power production in bus n.
V_n	Voltage magnitude at bus n.
δ	Rotor angle of the one-machine infinite-bus (OMIB) equivalent.
δ_i	Rotor angle of generator i.
θ_n	Voltage angle at bus n.
ω	Rotor speed of the OMIB equivalent.
ω_i	Rotor speed of generator i.

C. Constants

a_i	Constant cost coefficient of generator i.
b_i	Lineal cost coefficient of generator i.
c_i	Quadratic cost coefficient of generator i.
$I_{nm}^{\max}$	Maximum current magnitude through line nm.
P_{Dn}	Total active power consumed in bus n.
$P_{Gi}^{\max}$	Capacity of generator i.
$P_{Gi}^{\min}$	Minimum power output of generator i.
Q_{Dn}	Total reactive power consumed in bus n.
$Q_{Gi}^{\max}$	Maximum reactive power limit of generator i.
$Q_{Gi}^{\min}$	Minimum reactive power limit of generator i.
$V_n^{\max}$	Maximum voltage magnitude at bus n.
$V_n^{\min}$	Minimum voltage magnitude at bus n.
$\delta^{\max}$	Rotor angle limit of the OMIB equivalent.

D. Parameters

B_{ij}	Element ij of the reduced susceptance matrix.
G_{ij}	Element ij of the reduced conductance matrix.
M_C	Total inertia coefficient of the critical machine group.
M_i	Inertia coefficient of generator i.
M_{NC}	Total inertia coefficient of the noncritical machine group.

$\mathbf{Y}_{\text{bus}}$ Reduced admittance matrix.

$\mathbf{Y}_{Dn}$ Equivalent load admittance in bus n.

x'_{di} Transient reactance of generator i.

Δt Integration time step.

δ_r Return angle of the OMIB equivalent.

δ_u Instability limit angle of the OMIB equivalent.

Ω_b Frequency rating.

E. Sets

$\mathcal{G}$ Set of online generators.

$\mathcal{G}_C$ Set of critical machines.

$\mathcal{G}_n$ Set of online generators located at bus n.

$\mathcal{G}_{NC}$ Set of noncritical machines.

$\mathcal{N}$ Set of buses.

$\mathcal{T}$ Set of time steps.

Θ_n Set of buses connected to bus n.

I. INTRODUCTION

A. Motivation

The optimal power flow (OPF) is an appropriate and well-established tool to identify the control actions (e.g., generating unit dispatching or redispatching actions) needed to ensure an appropriate security level prior to real-time operation.

The use of a security constrained OPF is increasingly needed nowadays in stressed electric energy systems, which operate under market rules. Thus, there exists a significant need to develop OPF models that incorporate a diverse type of security constraints to guarantee an appropriate security level.

On the other hand, to study the transient stability under a major disturbance requires generally cumbersome time-domain simulations. Also, to incorporate transient stability constraints within an OPF model poses the challenge of marrying time-simulation and optimization. We propose an efficacious procedure to achieve this marriage.

B. Literature Review

The transient stability constrained OPF (TSC-OPF) is a nonlinear semi-infinite optimization problem that includes algebraic constraints and differential equations. For this reason, standard mathematical programming techniques cannot be directly applied and a variety of *ad hoc* algorithms has been proposed. A critical review of several approaches proposed for solving the TSC-OPF problem can be found in [1].

Two main aspects differentiate the TSC-OPF models that have been proposed in the literature, namely, 1) how the transient stability constraints are embedded in the OPF problem; and 2) how the transient stability assessment is approached. A brief literature review of these two aspects follows.

1) Inclusion of Transient Stability Constraints in the OPF: In [2]–[4], the authors convert the original TSC-OPF into an optimization problem via a constraint transcription based on functional transformation techniques. This approach seems to be a promising method to solve large systems. In [5] and [6], the authors convert the power system transient stability model into an algebraic set of equations for each time step of the time-domain simulation. This set of algebraic equations is introduced in the OPF as transient stability constraints. The size of the resulting problem is typically large. Also, in [7], this model is extended to consider multiple contingencies. The number of constraints is significantly reduced by using the reduced admittance matrix in [7] and [8]. In [9], [10], and [11], the transient stability assessment is solved and the results are used to determine a bound on the active power generation of a group of "critical machines" within the OPF problem. The main advantages of this approach are the compatibility with any dynamic model of the system and a low computational burden, while the main drawback is that obtaining an optimal solution cannot be guaranteed.

2) Transient Stability Assessment: The transient stability assessment can be done through time-domain simulation [2], [6]–[8], [10], [12]; transient energy function (TEF) and potential energy boundary surface (PEBS) [5], [13], [14], [15]; or hybrid methods [9], [16]–[19]. The time-domain simulation allows taking into account the full system dynamic model and consists in checking that inter-machine rotor angle deviations lie within a specific range of values. Unfortunately, this range is system, if not operating point, dependent and, in general, is not easy to establish. The methods based on the transient energy function are able to highly reduce computational times. However, the main limitation on the applicability of these methods lies in the construction of a suitable Lyapounov function and in the definition of the stability domain. Hybrid methods allow combining the advantages of time-domain simulation and transient energy function methods and avoiding some drawbacks. This paper uses the hybrid method proposed in [9].

C. Model Features

We strive to simplify the constraints related to the time-domain simulation while retaining the essential features characterizing this time simulation, which allows ruling out transients instabilities. To do this, we reduce the original multi-machine model to a two-machine model using the concept of SIngle Machine Equivalent (SIME), well documented in [20]. This two-machine model is further reduced to a one-machine infinite-bus (OMIB) equivalent, following well-established procedures [17], [20]. A bound calculated through appropriate time-domain simulations is imposed on the angle of the single equivalent machine to ensure transient stability.

The considered TSC-OPF includes, among others, the pre-fault power flow equations, technical bounds on generators, buses and lines, discrete-time swing equations for all the machines of the system (reproducing the actual time-domain simulation), as well as the transient stability bound on the angle of the single equivalent machine. The objective function to be minimized is the cost incurred as a result of dispatching or redispatching available generating units.

TABLE I
SOME ANGLE LIMITS FOR STABILITY ANALYSIS USED IN THE LITERATURE

Reference	Stability limit ($\delta_{ij}^{\max}$ or similar)
[3], [5], [13]	change of sign of PEBS
[6], [7], [8], [12]	$100°$
[10]	π
[4]	$2\pi/3$
[2]	$4\pi/5$
[11]	3π

The SIME approach is also used in [9], where the authors perform a separate analysis based on the OMIB only to estimate the power to shift from critical to noncritical machines [20]. In this paper, we use the OMIB to determine the maximum angle excursion, and this information is embedded in the OPF problem to dispatch or redispatch generator powers. Thus, the proposed methodology is expected to be more accurate and more transparent to the market than the one presented in [9].

Most methods proposed in the literature use a heuristic limit on the rotor angle deviation for identifying a transient instability. Table I shows some of such limits. The SIME-based stability constraint proposed in this paper detects the very instability mechanisms instead of observing the effect of the latter and thus allows adaptively determining an appropriate value of the maximum rotor angle deviation to avoid a transient instability.

Solving an OPF model requires the use of a nonlinear solver and accounting for nonconvexity. Currently available solvers (CONOPT [21], MINOS [22]) are robust and sufficiently efficient in terms of computing time to tackle OPFs. These solvers fully exploit sparse matrix techniques and can be started from different initial points so local minima are avoided. Alternatively to optimization solvers, heuristic procedures (e.g., [18] or [19]) can be used but at the cost of not being able to characterize precisely the quality of the solution attained. Thus, we advocate the use of state-of-the-art solvers such as CONOPT or MINOS and multiple runs using different initial solutions to solve OPFs.

D. Contributions

The main contributions of this paper are:
1) to develop transient stability constraints based on an effective hybrid method for transient stability assessment;
2) to provide a novel dispatching/redispatching OPF-based iterative methodology to ensure transient stability by identifying the minimal corrective actions to avoid first- and multi-swing instability.

E. Paper Organization

The remainder of the paper is organized as follows. Section II presents the dynamic model used for the machines of the system and the transient stability criterion. Section III provides the detailed mathematical formulation of the proposed TSC-OPF model, while Section IV describes the proposed dispatching/redispatching procedure. In Section V, three case studies based on the WECC nine-bus three-machine system, on the New England 39-bus ten-machine system, and on a 1228-bus, 292-machine system, are analyzed and discussed in detail. Section VI gives some conclusions.

II. SYSTEM MODEL AND TRANSIENT STABILITY CRITERION

A. Synchronous Machine Model

An advantage of the proposed technique is that any detailed models of the synchronous machine and its controls can be considered. In this paper, we use the classical model of the synchronous machine since it allows reducing the computational burden of the proposed approach while maintaining reliable results. Thus, the swing equations for the machine are represented by a constant emf behind a transient reactance [23]

$$\dot{\delta}_i = \Omega_b(\omega_i - 1), \quad \forall i \in \mathcal{G} \tag{1}$$

$$\dot{\omega}_i = \frac{1}{M_i}(P_{Gi} - P_{ei}), \quad \forall i \in \mathcal{G}. \tag{2}$$

In (2), the mechanical power P_{Gi} is considered constant, i.e., fast valving or generator power shedding are not considered.

If the loads are approximated as constant impedances, the equivalent load admittance at bus n is

$$\mathbf{Y}_{Dn} = \frac{P_{Dn}}{V_n^2} - j\frac{Q_{Dn}}{V_n^2} \tag{3}$$

and the original network can be transformed into an equivalent reduced network whose nodes are only the internal generator nodes [23]. The admittance matrix of the reduced network is called *reduced* admittance matrix and can be used to define the electrical power of the generators. Hence, the electrical power P_{ei} in (2) can be written as

$$P_{ei} = E_i' \sum_j E_j'[B_{ij}\sin(\delta_i - \delta_j) + G_{ij}\cos(\delta_i - \delta_j)]. \tag{4}$$

The proposed formulation allows reducing the number of variables and constraints of the OPF model, because bus voltage magnitudes and phases as well as the equations of current injections at network buses are not needed in (4). Furthermore, considering the results of the case studies presented in this paper, we conclude that the computing time of the OPF model based on the full admittance matrix is generally significantly higher than the one required by the proposed OPF problem. This increase in computing time can be due to the higher number of constraints and variables and difficulties in finding an initial feasible solution.

The reduced admittance matrix can be used also with a detailed generator model, as far as the loads are represented as constant impedances and the admittance matrix reduction is stopped at the machine buses and not extended to the fictitious internal node of the classical machine model.

B. Transient Stability Criterion

The transient stability criterion used in this paper is based on the SIME method [9], [20]. SIME is a transient stability analysis technique based on a simple but effective and well-proved

technique. For each step of the time-domain simulation, SIME divides the multi-machine system into two groups, 1) the group of machines that are likely to lose synchronism (*critical machines*) and 2) all other machines (*noncritical machines*). The maximum difference between two adjacent rotor angles, say $\delta_i - \delta_j$, indicates the frontier between the two machine groups, as follows. All generators whose rotor angles are greater than δ_i are part of the critical machine group, while all generators whose rotor angles are lower than δ_j are part of the noncritical machine group. These two groups are replaced by an OMIB equivalent system, whose transient stability is determined by means of the equal-area criterion (EAC). Finally, SIME establishes a set of stability conditions based on the equivalent OMIB parameters and on the EAC. A detailed description of the SIME method is given in [20], whereas a brief summary can be found in [24]. In the sequel, the SIME method is illustrated through some examples.

If the simulation is unstable, SIME provides information about which are the critical machines, the time t_u and the rotor *unstable* angle δ_u for which the instability conditions are reached. Similarly, if a simulation is first-swing stable, SIME provides the time t_r and the rotor *return* angle δ_r for which the OMIB equivalent meets the first-swing stability conditions. We use SIME criteria to define transient stability limits in the OPF problem, as described in Section IV.

III. TSC-OPF MODEL DESCRIPTION

A. Objective Function

If the TSC-OPF is used as a dispatching tool, the objective function $z = f(\cdot)$ represents the operating cost of power production:

$$f(P_{Gi}) = \sum_{i \in \mathcal{G}} a_i + b_i P_{Gi} + c_i P_{Gi}^2 \qquad (5)$$

where P_{Gi} is the active power generation of generator i and a_i, b_i, and c_i are its cost coefficients.

If the TSC-OPF is used as a redispatching tool, the objective function $f(\cdot)$ represents the cost of power adjustments as

$$f\left(\Delta P_{Gi}^{\mathrm{up}}, \Delta P_{Gi}^{\mathrm{down}}\right) = \sum_{i \in \mathcal{G}} r_{Gi}^{\mathrm{up}} \Delta P_{Gi}^{\mathrm{up}} + r_{Gi}^{\mathrm{down}} \Delta P_{Gi}^{\mathrm{down}} \quad (6)$$

where $\Delta P_{Gi}^{\mathrm{up}}$ and $\Delta P_{Gi}^{\mathrm{down}}$ are the power adjustments of generator i and r_{Gi}^{down} and r_{Gi}^{up} are the prices offered by the generator to decrease and increase its power dispatch for security purposes, respectively. In this case, the active generation powers P_{Gi} are defined by

$$P_{Gi} = P_{Gi}^{\mathrm{A}} + \Delta P_{Gi}^{\mathrm{up}} - \Delta P_{Gi}^{\mathrm{down}}, \quad \forall i \in \mathcal{G} \qquad (7)$$

where P_{Gi}^{A} represents the base case active generation power of generator i. The power adjustments need the following additional constraints:

$$\Delta P_{Gi}^{\mathrm{up}} \geq 0, \Delta P_{Gi}^{\mathrm{down}} \geq 0, \quad \forall i \in \mathcal{G}. \qquad (8)$$

Note that (6) establishes that any change from the base case implies a payment to the agents involved [25].

B. Power Flow Equations

The power flow equations are defined by the active and reactive power balances at all buses:

$$P_{Gn} - P_{Dn} = \sum_{m \in \Theta_n} P_{nm}(\cdot), \quad \forall n \in \mathcal{N} \qquad (9)$$

$$Q_{Gn} - Q_{Dn} = \sum_{m \in \Theta_n} Q_{nm}(\cdot), \quad \forall n \in \mathcal{N} \qquad (10)$$

where the powers on the left-hand side of each equation are defined as

$$P_{Gn} = \sum_{i \in \mathcal{G}_n} P_{Gi}, \quad \forall n \in \mathcal{N} \qquad (11)$$

$$Q_{Gn} = \sum_{i \in \mathcal{G}_n} Q_{Gi}, \quad \forall n \in \mathcal{N}. \qquad (12)$$

C. Technical Limits

The power production is limited by the capacity of the generators

$$P_{Gi}^{\mathrm{min}} \leq P_{Gi} \leq P_{Gi}^{\mathrm{max}}, \quad \forall i \in \mathcal{G} \qquad (13)$$

$$Q_{Gi}^{\mathrm{min}} \leq Q_{Gi} \leq Q_{Gi}^{\mathrm{max}}, \quad \forall i \in \mathcal{G}. \qquad (14)$$

The bus voltages magnitudes must be within the operating limits

$$V_n^{\mathrm{min}} \leq V_n \leq V_n^{\mathrm{max}}, \quad \forall n \in \mathcal{N}. \qquad (15)$$

The current flow through all series elements of the network must be below thermal limits:

$$I_{nm}(\cdot) \leq I_{nm}^{\mathrm{max}}. \qquad (16)$$

D. Initial Values of Machine Rotor Angles and emf Magnitudes

The initial values of generator rotor angles δ_i^0 and emf E_i' are obtained from the system pre-fault steady-state conditions as follows:

$$\frac{E_i' V_n \sin\left(\delta_i^0 - \theta_n\right)}{x_{di}'} - P_{Gi} = 0, \quad \forall i \in \mathcal{G}_n \qquad (17)$$

$$\frac{E_i' V_n \cos\left(\delta_i^0 - \theta_n\right) - V_n^2}{x_{di}'} - Q_{Gi} = 0, \quad \forall i \in \mathcal{G}_n. \quad (18)$$

Furthermore, since the pre-fault is a steady-state condition, one has

$$\omega_i^0 = 1, \quad \forall i \in \mathcal{G}. \quad (19)$$

E. Discrete Swing Equations

The swing equations (1) and (2) are discretized using the trapezoidal rule. Hence, generator rotor angles and speeds for a generic time step $(t + 1)$ are defined by the following equations:

$$\delta_i^{t+1} - \delta_i^t - \frac{\Delta t}{2} \Omega_b \left(\omega_i^{t+1} + \omega_i^t - 2\right) = 0$$
$$\forall t \in \mathcal{T}, \forall i \in \mathcal{G} \quad (20)$$

$$\omega_i^{t+1} - \omega_i^t - \frac{\Delta t}{2} \frac{1}{M_i} \left(P_{Gi} - P_{ei}^{t+1} + P_{Gi} - P_{ei}^t\right) = 0$$
$$\forall t \in \mathcal{T}, \forall i \in \mathcal{G} \quad (21)$$

where

$$P_{ei}^t = E_i' \sum_j E_j' \left[B_{ij}^t \sin\left(\delta_i^t - \delta_j^t\right) + G_{ij}^t \cos\left(\delta_i^t - \delta_j^t\right)\right]. \quad (22)$$

Note that the reduced admittance matrix depends on the network topology. Hence, in (22), the values of B_{ij}^t and G_{ij}^t are different for the during-fault and post-fault states, and consequently depend on time.

F. Transient Stability Limit

For each time step, the equivalent OMIB rotor angle must be below the instability limit provided by SIME:

$$\delta^t \leq \delta^{\max}, \quad \forall t \in \mathcal{T} \quad (23)$$

where $\mathcal{T}$ is as small as possible to reduce computing time but larger than the instability time t_u as defined by the SIME method. The inequality (23) is the main constraint that forces redispatching and is always binding. The dual variable μ associated with (23) indicates the sensibility of the objective function z with respect to $\delta^{\max}$:

$$\mu = \frac{dz}{d\delta^{\max}} \quad (24)$$

and is thus a measure of the impact of the stability constraints on the total dispatching or redispatching cost. The equivalent OMIB rotor angle is computed as

$$\delta^t = \frac{1}{M_C} \sum_{i \in \mathcal{G}_C} M_i \delta_i^t - \frac{1}{M_{NC}} \sum_{i \in \mathcal{G}_{NC}} M_i \delta_i^t \quad (25)$$

where

$$M_C = \sum_{i \in \mathcal{G}_C} M_i \text{ and } M_{NC} = \sum_{i \in \mathcal{G}_{NC}} M_i. \quad (26)$$

It is worth observing that (23) is a stability constraint compatible with most solution methods that have been proposed in the literature. Thus, (23) can be used in conjunction with reduced or full admittance matrix, detailed or simplified generator model, etc. The TSC-OPF formulation that is used in this paper is just one possible way of implementing (23).

G. Other Constraints

The proposed OPF problem is completed with the following additional constraints:

$$-\pi \leq \theta_n \leq \pi, \quad \forall n \in \mathcal{N} \quad (27)$$
$$\theta_{\text{ref}} = 0. \quad (28)$$

Equation (27) is included to reduce the feasibility region, thus generally speeding up the convergence of the OPF problem.

H. Problem Formulation

The formulation of the OPF problem is summarized as follows:

$$\text{Minimize (5) or (6)}$$

subject to
1) power flow (9)–(10);
2) technical limits (13)–(16);
3) initial values of machine rotor angles and emf magnitudes (17)–(19);
4) discrete swing equations (20)–(21);
5) transient stability limit (23);
6) other constraints (27)–(28).

The above formulation can be easily extended to the multi-contingency case by including constraints (20)–(21) and (23) for each considered contingency.

IV. PROCEDURE TO ENSURE TRANSIENT STABILITY

Converting the whole time-domain simulation of the system transient stability model into a set of algebraic equations results in a very large number of equations to be included in an OPF. Solving such nonlinear OPF problem may require prohibitive computing times and prohibitive memory size, and may lead to convergence issues. To reduce the number of constraints, we use the reduced admittance matrix and constrain the OMIB equivalent trajectory only during the first swing of the system. The latter allows including the discretized transient stability equations (20)–(21) and (23) only for a few seconds after the fault occurrence.

The proposed procedure is as follows.
1) *Base case solution.* The base case solution can be obtained from an OPF problem that consists of minimizing (5) subjected to power flow (9)–(10), technical limits (13)–(16),

and constraints (27)–(28). If the procedure is used as a re-dispatching tool, the base case corresponds to a dispatching solution obtained by any suitable technique.

2) *Contingency analysis*. The contingency analysis consists in identifying, from a set of credible contingencies, the ones that lead the system to instability. This identification is carried out by means of a time-domain simulation complemented by SIME using a technique similar to the one in [24]. For first-swing unstable contingencies, SIME provides the sets of critical and noncritical machines and the instability limit (δ_u) for the OMIB equivalent. Equations (23) and (25) incorporate this information.

3) *Solve the TSC-OPF problem*. The OPF problem described in Section III-H is solved and the new generating powers and bus voltages are computed.

4) *Check the new solution*. A time-domain simulation that includes SIME is solved for the new operating point obtained at step 3. This simulation is necessary to check the transient stability of the new operating point. Three different cases can be encountered.

    a) The system is stable and the procedure stops.

    b) The system is first-swing unstable. This is due to the fact that the reduced admittance $\mathbf{Y}_{\text{bus}}$ used in the optimization problem has been calculated for the initial solution that exhibits different voltage values than the solution obtained at step 3 [see (3)]. Thus, the reduced admittance matrix is updated and the transient stability limit $\delta^{\max}$ is fixed to the new value of δ_u. The procedure continues at step 3.

    c) The system is multi-swing unstable. In this case, the OMIB equivalent has a return angle δ_r in the first swing. However, after some cycles, the system loses synchronism. The return angle value δ_r is used to define the new transient stability limit $\delta^{\max}$. In order to avoid multi-swing phenomena, $\delta^{\max}$ is set to $\delta_r - \Delta\delta$, i.e., $\delta^{\max}$ is fixed to a value smaller than δ_r. The value of the decrement $\Delta\delta$ is defined based on a heuristic criterion. Finally, the reduced admittance matrix $\mathbf{Y}_{\text{bus}}$ is updated. The procedure continues at step 3.

The flowchart depicted in Fig. 1 illustrates the proposed procedure.

Note that in the first iteration, the TSC-OPF problem is initialized with the base case solution while in the following iterations, the TSC-OPF problem is initialized with the solution of the previous iteration. Since the OPF problem is nonconvex, the solution for each iteration can be double-checked by starting from several different initial guesses. Starting points are obtained by randomly perturbing (using a normal distribution within a 20% range) the base-case solution or the solution of the previous OPF solved. In our simulations, we did not observe convexity problems, mainly due to the fact that the initial guess is close to the optimum.

We consider that one single harmful contingency is found at step 2. However, as discussed in Subsection III-H, multiple contingencies can be readily taken into account by including (20)–(21) and (23) for each contingency in the TSC-OPF problem. In what follows, we are concerned only with single-contingency scenarios.
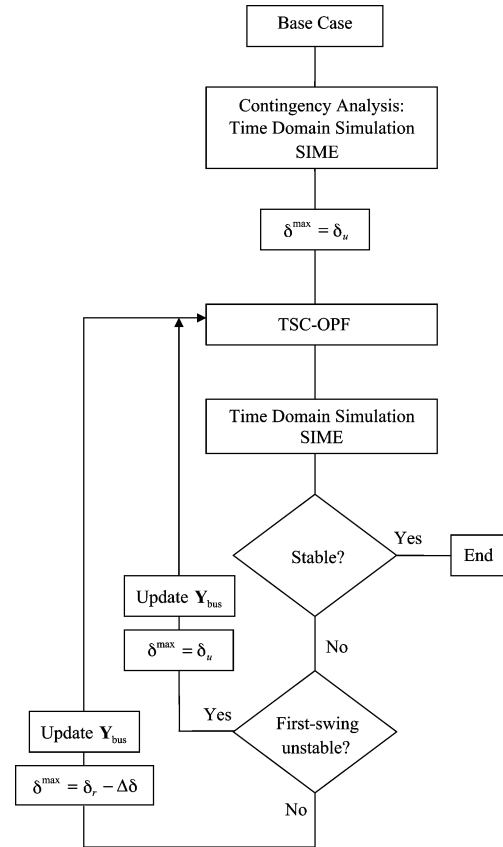

Fig. 1.   Flow chart of the proposed procedure.

There could be situations where the power shifts determined by the proposed procedure could modify the instability mode, i.e., change the set of critical/noncritical machines. This requires to include (23) and (25) for both the previous and the new instability mode.

V. CASE STUDIES

In this section, we present the result of a variety of case studies based on the WECC nine-bus, three-machine system; the New England 39-bus, ten-machine system; and a 1228-bus, 292-machine system. While the nine-bus and 39-bus systems are presented for the sake of comparison with existing literature [10], [19], the 1228-bus system is used for testing the proposed transient stability criterion in a real-world large-scale system. All simulations were carried out using Matlab 7.6 [26] and GAMS 22.7 [27]. For solving time-domain simulations, we used PSAT [28] that has been modified to include an embedded SIME algorithm. Finally, the proposed TSC-OPF problem has been solved using CONOPT [21].

The whole simulation time is 5 s for time-domain simulations, whereas the discretized dynamic equations are included for the first 2 s in the TSC-OPF problem. Setting $\mathcal{T} = [0, 2]$ s is sufficient to reveal first swing transient instabilities. However, performing time-domain simulation over 5 s guarantees that the system does not undergoes multi-swing instability.
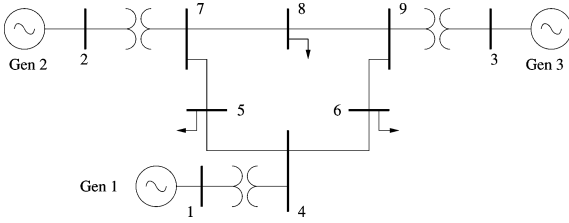
Fig. 2. One-line diagram of the WECC three-machine, nine-bus system.

A. WECC Nine-Bus, Three-Machine System

Fig. 2 shows the WECC three-machine, nine-bus system. The full dynamic data of this system can be found in [29], while generator cost data and limits are defined in [10] and [19]. In order to compare results with [10] and [19], we use the proposed technique as a dispatching TSC-OPF; thus, (5) is used as objective function.

In this case study, we consider the following two cases.

Case A: A three-phase-to-ground fault occurs at bus 7 and is cleared after 0.35 s by tripping line 7-5. This case corresponds to Case A of [10] and [19].

Case B: A three-phase-to-ground fault occurs at bus 9 and is cleared after 0.30 s by tripping line 9-6. This case corresponds to Case B of [10] and [19].

The base case solution is first-swing unstable for the contingencies of both cases, A and B. In case of multi-swing instability, we use $\Delta\delta = 1$ degree for computing the new value of $\delta^{\max}$. The time step used in these case studies is $\Delta t = 0.01$ s.

1) Case A: The equivalent OMIB for the base case solution is unstable since the rotor angle δ increases beyond the admissible angle $\delta_u = 160.44$ degrees after $t_u = 0.49$ s. Fig. 3 shows the unstable behavior of the base case OMIB equivalent and of rotor angle trajectories after the occurrence of the contingency and the subsequent fault clearing. After carrying out the steps of the procedure described in Section IV, the system becomes stable. The procedure requires three iterations to converge, as follows.

1) In the first iteration, the TSC-OPF solution is first-swing unstable, as shown in Fig. 4. The equivalent OMIB trajectory reaches the instability conditions at $t_u = 0.79$ s with an unstable angle $\delta_u = 152.28$ degrees.

2) In the second iteration, the TSC-OPF solution is multi-swing unstable: the equivalent OMIB trajectory shows a return angle $\delta_r = 150.55$ degrees in the first swing at $t_r = 0.74$ s but the system loses synchronism at $t_u = 2.63$ s. Fig. 5 confirms that this is a multi-swing case.

3) Finally, in the third iteration, the TSC-OPF solution is stable. Fig. 6 shows that the equivalent OMIB and rotor angle trajectories remain stable during the whole time-domain simulation. The OMIB return angle is $\delta_r = 149.51$ degrees in the first-swing at $t_r = 0.72$ s.

2) Case B: The OMIB equivalent for the base case solution is unstable after the occurrence of the contingency and the subsequent fault clearing. At $t_u = 0.32$ s, the rotor angle δ increases beyond the admissible angle $\delta_u = 171.16$ degrees, and thus,
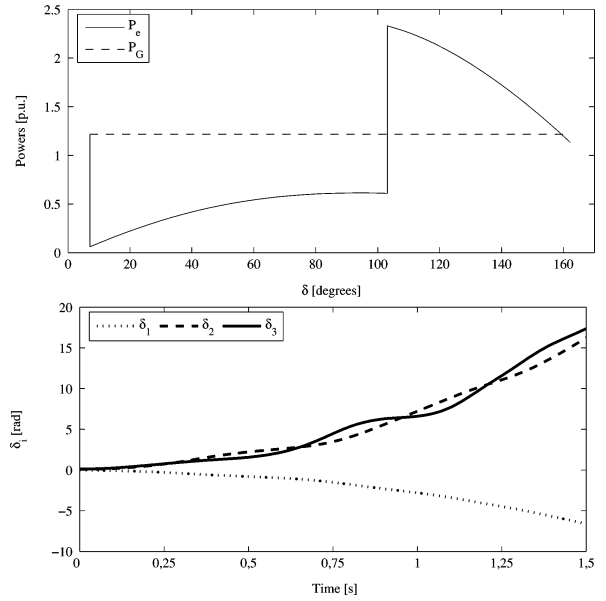

Fig. 3. Case A. OMIB plot and rotor angle trajectories for the WECC three-machine, nine-bus system: unstable base case.
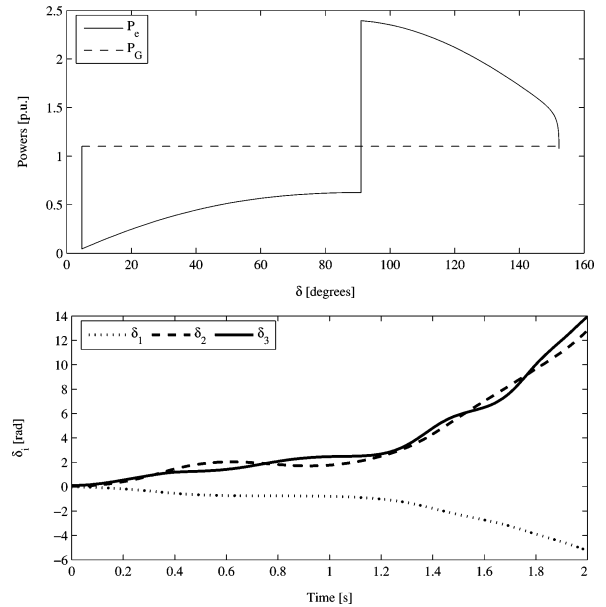

Fig. 4. Case A. OMIB plot and rotor angle trajectories for the WECC three-machine, nine-bus system: first iteration of the TSC-OPF procedure. The system shows first-swing instability.

the system loses synchronism. By applying the procedure described in Section IV, the resulting system recovers stability. In this case, the procedure requires two iterations to converge, as follows.

1) In the first iteration, the TSC-OPF solution is multi-swing unstable. The equivalent OMIB trajectory reaches the first-swing stability conditions at $t_r = 0.48$ s with a return angle $\delta_r = 166.19$ degrees but the system loses synchronism at $t_u = 1.45$ s.

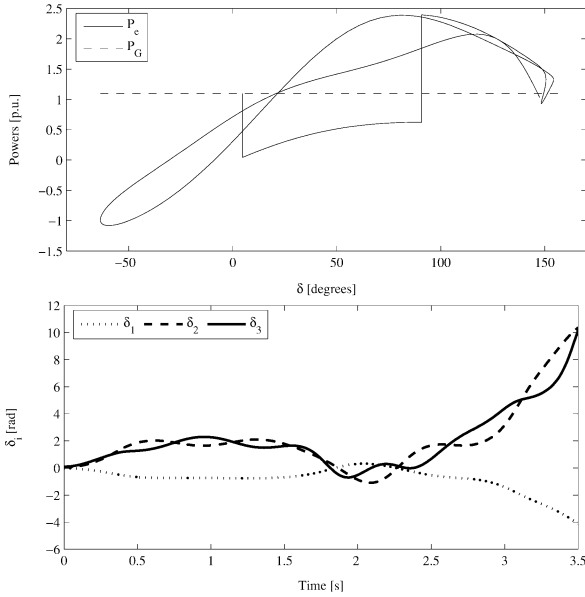2) In the second iteration, the TSC-OPF solution is stable. The equivalent OMIB trajectory remains stable during the

Fig. 5. Case A. OMIB plot and rotor angle trajectories for the WECC three-machine, nine-bus system: second iteration of the TSC-OPF procedure. The system shows multi-swing instability.
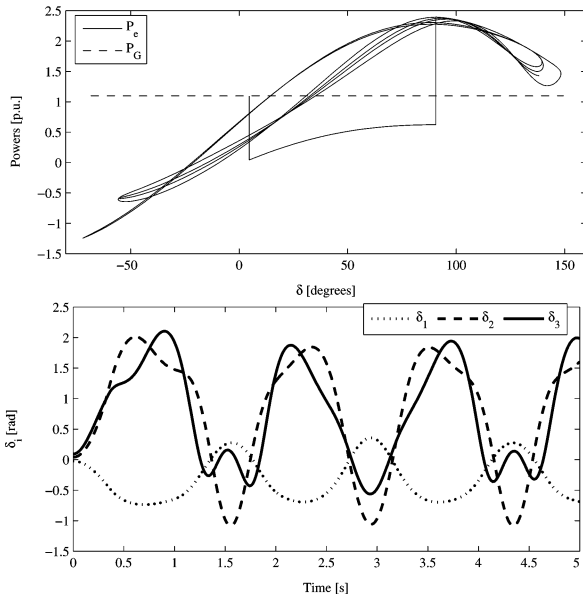

Fig. 6. Case A. OMIB plot and rotor angle trajectories for the WECC three-machine, nine-bus system: third and final iteration of the TSC-OPF procedure. The system is stable.

TABLE II
OPTIMAL SOLUTIONS FOR THE NINE-BUS, THREE-MACHINE SYSTEM

Generator	Base Case (MW)	Case A (MW)	Case B (MW)
G1	105.94	117.85	120.01
G2	113.04	103.50	121.13
G3	99.24	96.66	76.84
Cost ($/h)	1132.18	1134.01	1137.82

TABLE III
COMPARISON OF TOTAL COSTS FOR NINE-BUS, THREE-MACHINE SYSTEM

Case	TSC-OPF ($/h)	Ref. [19] ($/h)	Ref. [10] ($/h)
Base Case	1132.18	1132.30	1132.59
Case A	1134.01	1140.06	1191.56
Case B	1137.82	1147.77	1179.95
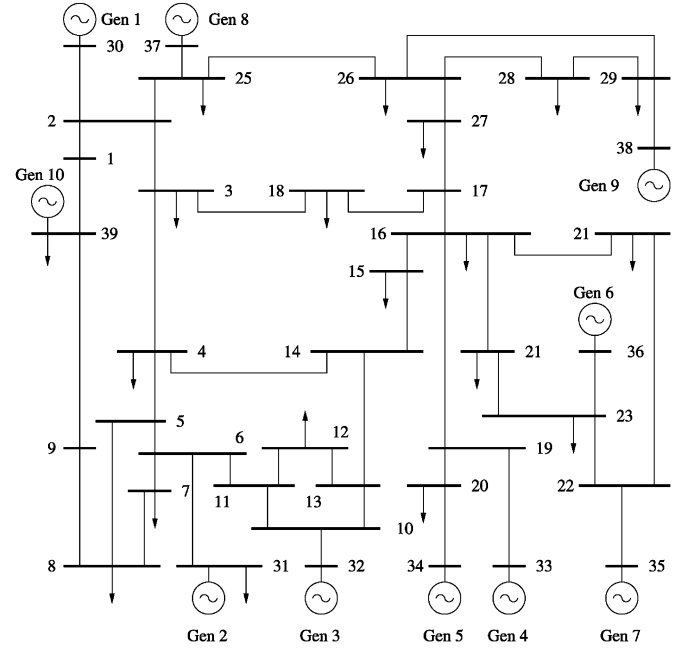
Fig. 7. One-line diagram of the New England ten-machine, 39-bus system.

whole time-domain simulation with a return angle $\delta_r = 165.14$ degrees in the first swing at $t_r = 0.49$ s.

The results of the case studies solved for the WECC system are summarized in Table II. This table shows the generated active powers for the base case and for cases A and B as obtained by implementing the proposed TSC-OPF-based procedure. Table II also shows the resulting total cost of the base case and cases A and B. As expected, the solutions of cases A and B are more expensive than the one pertaining to the base case.

For the sake of comparison, Table III provides the results obtained by means of the proposed TSC-OPF and the results obtained in [10] and [19]. In particular, Table III shows the total costs for the base case and for cases A and B. The proposed technique provides overall better or similar results than the other ones. The differences in the base case solutions are mainly due to truncation errors of the solvers and rounding of input data.

B. New England 39-Bus, Ten-Machine System

Fig. 7 shows the New England ten-machine, 39-bus system. The full dynamic data of this system can be found in [14], while generator cost data and limits are defined in [10] and [19]. As in the case of the WECC system, (5) is used as objective function in order to compare results with [10] and [19].

In this case study, we consider the following two cases.

Case C: A three-phase-to-ground fault occurs at bus 4 and is cleared after 0.25 s by tripping line 4–5. This case corresponds to Case C of [19] and Case E of [10].
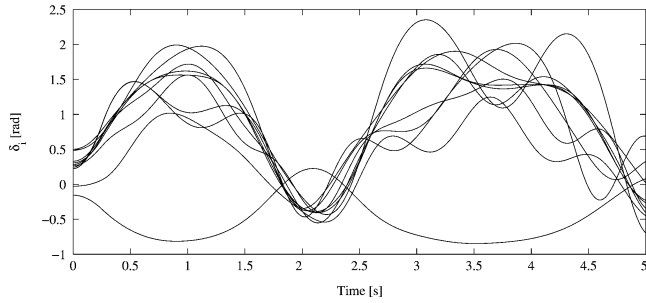
Fig. 8.   Case C. Stable trajectories of generator rotor angles for the New England 39-bus system.
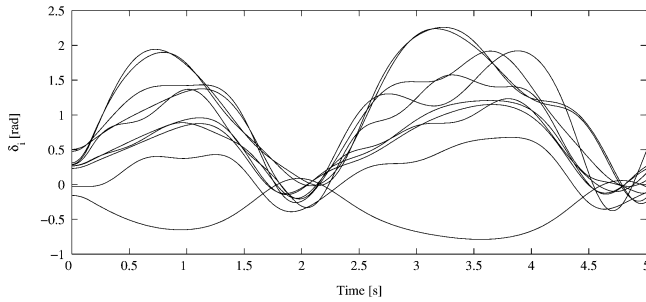

Fig. 9.   Case D. Stable trajectories of generator rotor angles for the New England 39-bus system.

Case D: A three-phase-to-ground fault occurs at bus 21 and is cleared after 0.16 s by tripping line 21–22. This case corresponds to Case D of [19].

Both cases C and D lead to a first-swing unstable base case solution, and it is thus necessary to modify the initial dispatching to stabilize the system. The time step used in these case studies is $\Delta t = 0.01$ s.

1) Case C: The equivalent OMIB for the base case solution is unstable after the occurrence of the contingency and the following fault clearing, since the rotor angle δ increases beyond the admissible angle $\delta_u = 145.26$ degrees after $t_u = 1.07$ s. The proposed TSC-OPF procedure stabilizes the system, as confirmed by Fig. 8.

2) Case D: This case is similar to the previous case C. The base case OMIB equivalent is unstable since the rotor angle δ increases beyond the admissible angle $\delta_u = 123.10$ degrees which is reached at $t_u = 1.05$ s. After processing the system through the proposed TSC-OPF methodology, the system recovers stability. The resulting stable trajectories of the machine rotor angles are depicted in Fig. 9.

In both cases C and D, after some iterations of the proposed technique, a multi-swing instability occurs. This instability is detected by the time-domain simulation. To avoid the multi-swing instability, further iterations are needed.

Table IV shows the generated active powers as well as the resulting total costs for the base case and for cases C and D as obtained by solving the proposed TSC-OPF-based procedure. The results confirm that the adjustments of the generated powers needed to stabilize the system make the solutions of cases C and D more expensive than that of the base case.

For comparison and completeness, Table V shows the total costs for the base case and cases C and D as obtained by using

TABLE IV
OPTIMAL SOLUTIONS FOR 39-BUS, TEN-MACHINE SYSTEM

Generator	Base Case (MW)	Case C (MW)	Case D (MW)
G1	242.39	245.38	245.94
G2	566.94	554.57	572.56
G3	642.73	630.71	648.11
G4	629.50	626.14	627.56
G5	507.90	506.08	505.91
G6	650.38	646.92	628.12
G7	557.99	554.49	539.01
G8	534.76	537.93	539.94
G9	829.37	829.28	833.38
G10	977.56	1007.89	998.56
Cost ($/h)	60918.66	60934.82	60937.85

TABLE V
COMPARISON OF COSTS FOR 39-BUS, TEN-MACHINE SYSTEM

Case	TSC-OPF ($/h)	Ref. [19] ($/h)	Ref. [10] ($/h)
Base Case	60918.66	60936.51	60992.88
Case C	60934.82	61021.04	61826.53
Case D	60937.85	60988.25	-

the proposed TSC-OPF procedure and the ones presented in [10] and [19]. Also in this case study, the proposed technique provides overall better or similar results than the other ones. As in the case of the WECC system, the differences in the base case solutions are due to numerical approximations.

C. A 1228-Bus, 292-Machine System

A 1228-bus, 1903-line/transformer, and 292-machine system is considered in this subsection to show that the proposed technique can be applied to a real-world power system. All machines are modeled using a second-order model. We assume that the initial power flow solution is the result of a market clearing procedure that does not include transient stability constraints. Fig. 10 shows the loss of synchronism of 11 machines following a three-phase short circuit cleared after 0.2 s. The base case OMIB equivalent is unstable since the rotor angle δ increases beyond the admissible angle $\delta_u = 157.75$ degrees which is reached at $t_u = 0.4375$ s.

We use the proposed technique as a redispatching tool, i.e., we use (6) as objective function. This way, the TSC-OPF problem minimizes the cost of shifting generation with respect to the initial operating point. The time step used in this case is $\Delta t = 0.1$ s. The whole procedure converges in just one iteration (no multi-swing shows up in this case). Assuming as a CPU time base the time necessary to solve one OPF problem without stability constraints [i.e., problem (6), (9)–(10), (13)–(16), and (27)–(28)] plus one time-domain simulation, the per unit CPU time required to solve this case study is 11.4. The resulting trajectories of generator rotor angles after redispatching are shown in Fig. 11.
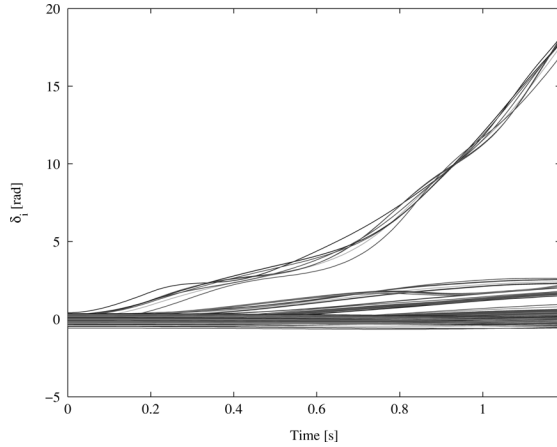
Fig. 10. Unstable trajectories of generator rotor angles for the 1228-bus system.
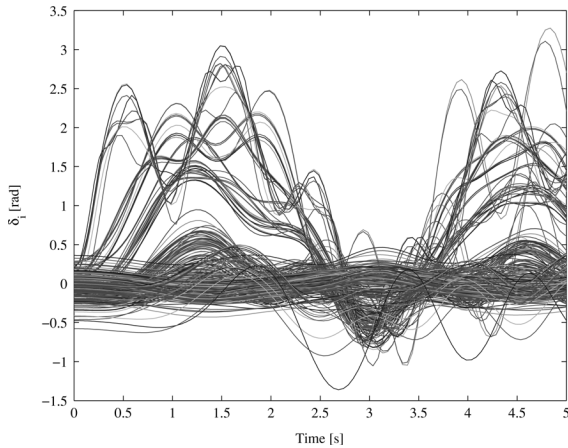

Fig. 11. Stable trajectories of generator rotor angles for the 1228-bus system.

TABLE VI
EFFECT OF $\Delta\delta$ PARAMETER ON SIMULATION TIMES
AND COSTS FOR THE 39-BUS, TEN-MACHINE SYSTEM

$\Delta\delta$ (deg.)	Case C			Case D		
	Iter. #	CPU (p.u.)	Cost ($/h)	Iter. #	CPU (p.u.)	Cost ($/h)
1	31	41.84	60934.82	37	57.39	60937.85
3	14	16.83	60939.03	13	20.39	60939.21
5	9	11.99	60937.37	8	13.05	60938.50

D. Concluding Remarks

As any stability constrained OPF procedure, the proposed TSC-OPF problem includes a variety of parameters that can be adjusted to improve computational performance, especially in terms of computing time. In this subsection, we focus on two parameters, i.e., the variation $\Delta\delta$ that is used at each iteration in case of multi-swing instability, and the time step Δt used for the numerical time integration embedded in the OPF problem. For the sake of illustration, in the following paragraphs, we consider the WECC case studies C and D.

Effect of Varying $\Delta\delta$: Table VI provides number of iterations, per unit CPU times, and total costs obtained for $\Delta\delta = 1, 3$ and 5

TABLE VII
EFFECT OF Δt PARAMETER ON SIMULATION TIMES
AND COSTS FOR THE 39-BUS, TEN-MACHINE SYSTEM

Δt (s)	Case C			Case D		
	Iter. #	CPU (p.u.)	Cost ($/h)	Iter. #	CPU (p.u.)	Cost ($/h)
0.01	31	41.84	60934.82	37	57.39	60937.85
0.025	27	21.19	60935.40	32	24.01	60936.93
0.05	20	11.38	60935.72	23	13.38	60938.68
0.1	9	5.19	60937.73	11	6.34	60938.48

degrees, respectively. CPU times are normalized with respect to the time necessary to solve one OPF problem without stability constraints plus one time-domain simulation. Each iteration involves steps 3 and 4 of the procedure described in Section IV. The results show that decreasing $\Delta\delta$ does not improve notably the total cost of the dispatching procedure while it significantly increases the computational time.

Effect of Varying Δt: Table VII shows that different time steps Δt can lead to similar total costs with significantly different simulation times. From our experience, we conclude that time steps up to 0.1 s provide an appropriate trade-off between accuracy and efficiency for the model used and the technique proposed.

Finally, note that the SIME-based transient stability constraint is compatible with any OPF formulation.

VI. CONCLUSION

This paper provides a methodology to ensure transient stability. It relies on an OPF model with embedded transient stability constraints. These constraints are based on SIME method and ensure transient stability of the system against major disturbances, e.g., faults and/or line outages. In addition to power flow constraints and bounds, the resulting OPF model includes discrete time equations describing the time evolution of all machines in the system and a stability constraint on the OMIB defined by SIME. The proposed technique is suited for both dispatching or redispatching procedures.

The variety of case studies that are discussed in the paper shows that the proposed TSC-OPF procedure is reliable and generally provides more economical results than other existing techniques.

An advantage of the proposed technique is the fact that additional details can be incorporated by taking into account alternative device models and/or adding different transient stability constraints. These modifications and their effects on the accuracy of the results will be investigated in future work on this topic.

REFERENCES

[1] H. Xin, D. Gan, Y. Li, T. S. Chung, and J. Qiu, "Transient stability preventive control and optimization via power system stability region analysis," in *Proc. IEEE Power Eng. Soc. General Meeting*, Jun. 2006, vol. 1.

[2] L. Chen, Y. Tada, H. Okamoto, R. Tanabe, and A. Ono, "Optimal operation solutions of power systems with transient stability constraints," *IEEE Trans. Circuits Syst. I, Fundam. Theory Appl.*, vol. 48, no. 3, pp. 327–339, Mar. 2001.

[3] Y. Sun, Y. Xinlin, and H. F. Wang, "Approach for optimal power flow with transient stability constraints," *Proc. Inst. Elect. Eng., Gen., Transm., Distrib.*, vol. 151, no. 1, pp. 8–18, Jan. 2004.

[4] Y. Xia, K. W. Chan, and M. Liu, "Direct nonlinear primal-dual interior-point method for transient stability constrained optimal power flow," *Proc. Inst. Elect. Eng., Gen., Transm., Distrib.*, vol. 152, no. 1, pp. 11–16, Jan. 2005.

[5] M. L. Scala, M. Trovato, and C. Antonelli, "On-line dynamic preventive control: An algorithm for transient security dispatch," *IEEE Trans. Power Syst.*, vol. 13, no. 2, pp. 601–609, May 1998.

[6] D. Gan, R. J. Thomas, and R. D. Zimmerman, "Stability-constrained optimal power flow," *IEEE Trans. Power Syst.*, vol. 15, no. 2, pp. 535–540, May 2000.

[7] Y. Yuan, J. Kubokawa, and H. Sasaki, "A solution of optimal power flow with multicontingency transient stability constraints," *IEEE Trans. Power Syst.*, vol. 18, no. 3, pp. 1094–1102, Aug. 2003.

[8] D. Layden and B. Jeyasurya, "Integrating security constraints in optimal power flow studies," in *Proc. IEEE Power Eng. Soc. General Meeting*, Jun. 2004, vol. 1.

[9] D. Ruiz-Vega and M. Pavella, "A comprehensive approach to transient stability control: Part I—Near optimal preventive control," *IEEE Trans. Power Syst.*, vol. 18, no. 4, pp. 1446–1453, Nov. 2003.

[10] T. B. Nguyen and M. A. Pai, "Dynamic security-constrained rescheduling of power systems using trajectory sensitivities," *IEEE Trans. Power Syst.*, vol. 18, no. 2, pp. 848–854, May 2003.

[11] D. Z. Fang, Y. Xiaodong, Y. Jingqiang, Y. Shiqiang, and Z. Yao, "An optimal generation rescheduling approach for transient stability enhancement," *IEEE Trans. Power Syst.*, vol. 22, no. 1, pp. 386–394, Feb. 2007.

[12] D. Chattopadhyay and D. Gan, "Market dispatch incorporating stability constraints," *Int. J. Elect. Power Energy Syst.*, vol. 23, no. 6, pp. 459–469, Aug. 2001.

[13] S. Bruno, E. De Tuglie, M. L. Scala, and P. Scarpellini, "Transient security dispatch for the concurrent optimization of plural postulated contingencies," *IEEE Trans. Power Syst.*, vol. 17, no. 3, pp. 707–714, Aug. 2002.

[14] M. A. Pai, *Energy Function Analysis for Power System Stability*. Norwell, MA: Kluwer, 1989.

[15] A. A. Fouad and V. Vittal, *Power System Transient Stability Analysis Using the Transient Energy Function Method*. Englewood Cliffs, NJ: Prentice-Hall, 1992.

[16] G. A. Maria, C. Tang, and J. Kim, "Hybrid transient stability analysis," *IEEE Trans. Power Syst.*, vol. 5, no. 2, pp. 384–393, May 1990.

[17] M. Pavella, "Generalized one-machine equivalents in transient stability studies," *IEEE Power Eng. Rev.*, vol. 18, no. 1, pp. 50–52, Jan. 1998.

[18] X. Zhang, R. W. Dunn, and F. Li, "Stability constrained optimal power flow in a practical balancing market," in *Proc. IEEE Power Eng. Soc. General Meeting*, Jun. 2007, vol. 2.

[19] H. R. Cai, C. Y. Chung, and K. P. Wong, "Application of differential evolution algorithm for transient stability constrained optimal power flow," *IEEE Trans. Power Syst.*, vol. 23, no. 2, pp. 719–728, May 2008.

[20] M. Pavella, D. Ernst, and D. Ruiz-Vega, *Transient Stability of Power Systems: A Unified Approach to Assessment and Control*. Norwell, MA: Kluwer, 2000.

[21] A. S. Drud, *GAMS/CONOPT*. Bagsvaerd, Denmark: ARKI Consulting and Development, 1996. [Online]. Available: http://www.gams.com/.

[22] B. A. Murtagh, M. A. Saunders, W. Murray, P. E. Gill, R. Raman, and E. Kalvelagen, GAMS/MINOS: A Solver for Large-Scale Nonlinear Optimization Problems, 2002. [Online]. Available: http://www.gams.com/.

[23] P. M. Anderson and A. A. Fouad, *Power System Control and Stability*. Ames, IA: Iowa State Univ. Press, 1977.

[24] D. Ernst, D. Ruiz-Vega, M. Pavella, P. M. Hirsch, and D. Sobajic, "A unified approach to transient stability contingency filtering, ranking and assessment," *IEEE Trans. Power Syst.*, vol. 16, no. 3, pp. 435–443, Aug. 2001.

[25] A. J. Conejo, F. Milano, and R. Garcia-Bertrand, "Congestion management ensuring voltage stability," *IEEE Trans. Power Syst.*, vol. 21, no. 1, pp. 357–364, Feb. 2006.

[26] The MathWorks, Inc., Matlab Programming, 2005. [Online]. Available: http://www.mathworks.com.

[27] A. Brooke, D. Kendrick, A. Meeraus, R. Raman, and R. E. Rosenthal, *GAMS, a User's Guide*. Washington, DC: GAMS Development Corp., Dec. 1998. [Online]. Available: http://www.gams.com/.

[28] F. Milano, "An open source power system analysis toolbox," *IEEE Trans. Power Syst.*, vol. 20, no. 3, pp. 1199–1206, Aug. 2005.

[29] P. W. Sauer and M. A. Pai, *Power System Dynamics and Stability*. Upper Saddle River, NJ: Prentice-Hall, 1998.

Rafael Zárate-Miñano (S'05) received the Electrical Engineering degree from the University of Castilla-La Mancha, Ciudad Real, Spain, in April 2005. He is currently pursuing the Ph.D. degree at the University of Castilla-La Mancha.

His research interests are stability, electricity markets, sensitivity analysis, optimization, and numerical methods.

Thierry Van Cutsem (F'05) received the electrical-mechanical engineering degree and the Ph.D. degree from the University of Liège, Liège, Belgium.

Since 1980, he has been with the Fund for Scientific Research (FNRS), of which he is now a Research Director. He is also an Adjunct Professor at the University of Liège. His research interests are in power system dynamics, stability, security, simulation, and optimization, in particular voltage stability and security.

Federico Milano (M'03–SM'09) received the M.S. degree and the Ph.D. degree from the University of Genoa, Genoa, Italy, in 1999 and 2003, respectively.

In 2001–2002, he worked at the University of Waterloo, Waterloo, ON, Canada, as a Visiting Scholar. He is currently an Associate Professor at the University of Castilla-La Mancha, Ciudad Real, Spain. His research interests include voltage stability, electricity markets, and computer-based power system modeling.

Antonio J. Conejo (F'04) received the M.S. degree from the Massachusetts Institute of Technology, Cambridge, in 1987 and the Ph.D. degree from the Royal Institute of Technology, Stockholm, Sweden, in 1990.

He is currently a full Professor at the Universidad de Castilla-La Mancha, Ciudad Real, Spain. His research interests include control, operations, planning and economics of electric energy systems, as well as statistics and optimization theory and its applications.